INTERNATIONAL ATOMIC ENERGY AGENCY
UNITED NATIONS EDUCATIONAL, SCIENTIFIC AND CULTURAL ORGANIZATION

INTERNATIONAL CENTRE FOR THEORETICAL PHYSICS
34100 TRIESTE (ITALY) - P.O.B. 586 - MIRAMARE - STRADA COSTIERA 11 - TELEPHONES: 2 4281/2/3/4/5/6
CABLE: CENTRATOM - TELEX 460392-1

SMR/113 - 25

AUTUMN COLLEGE

ON

THE TROPOSPHERE, STRATOSPHERE AND MESOSPHERE

10 September - 19 October 1984

Annex II to SMR/113 - 1

(THE MST RADAR TECHNIQUE)

J. ROTTGER

EISCAT Scientific Association
Box 705
S-981 27 Kiruna
Sweden

Table I OPERATIONAL AND PLANNED MST/ST/IS RADARS (NOVEMBER 1983)

facil'	mode	lat./long. deg.	freq. MHz	ave.power kW	min.pulse width μs	duty cycle (max.)%	antenna aperture (eff.)m²	antenna beam width	antenna configuration	antenna mode	steerability	status	ref.
Arecibo/Puerto Rico	IS, ST	19N,67W	430	120	1	6	50000	0.17°	circ.dish	DB	20°(m)	op	(1)
" / "	MST		46.8	1	1	2	50000	1.7°	"	DB	"	ce	
Buckland Park/Australia	(M)ST	35S,138E	54.1	0.4	7	0.7	7500	3.2°	PAC,PAY	DB,SA	15°(1)	(op)	(2)
Chung-Li/Taiwan	(M)ST	25N,121E	52	4	1	2	2500	5°	PAY	DB,SA	15°(2)	ce	(3)
EISCAT/	IS,ST	70N (67N)	933.5	250	2	12.5	520	0.6°	3 circ.dishes	DB	80°(m),tristat.	op	(4a)
North Scandinavia	IS,ST	19E (27E)	224	600	2	12.5	3300	0.6°,1.7°	cyl.dish	DB	30°,60°,20°(m)	ce	(4b)
Equatorial Pacific	ST (3x)	(0,150E)	49.8	0.2	5	(2)	(5000)	(5°)	PAC	DB	15°(2)	pl/ce	(5)
India	MST	—	45-55	60	1	2.5	20000	3°	PAC	DB	20°(2)	pl	(6)
Jicamarca/Peru	MST,IS	12S,72W	49.9	200	(1)	5	80000	1.0°	PAC	DB,SA	3°(m)	op	(7)
LSEET/France	ST	43N,5E	47.0	1	2	1.7	3x2000	5°	PAC	DB	15°(2)	ce	(8)
Millstone Hill/USA	IS,ST	43N,72W	440	30	2	1.6	1640	1°	circ.dish	DB	<80°(m)	op	(9)
MU/Japan	MST,(IS)	35N,136E	46.5	50	1	5	8330	3.6°	PAY	DB,SA	30°(m)	(op)	(10)
Penn.State/USA	ST (3x)	41N,78W	48-50	1	4	2	2500	5°	PAC	DB	15°(2)	pl	(11)
Platteville/USA	ST (4x)	40N,105W	49.8	1	4	1.7	2000	5°	PAC	DB	15°(2)	op/rt	(12)
Poker Flat/USA	MST	65N,147W	49.9	128	2	2	40000	1.4°	PAC	DB	15°(2)	op/rt	(13)
PROUST/France	ST	45N,2E	935	(~10)	4 (0.2)		2000 (95)		2 dishes	DB	bistatic	(pl)	(14)
Sondre Stromfjord/Greenland	IS,ST	67N,51W	1290	100	(1)	3	420	0.5°	circ.dish	DB	90°(m)	op	(15)
SOUSY/Germany	MST	52N,10E	53.5	24	1	4	3200	5°	PAY	DB,SA	12.5°(m)	op	(16a)
" /Norway	MST	69N,16E	53.5	8	1	4	8800	3°	PAY	DB	4.0°(2),5.6°	op	(16b)
Sunset/USA	ST	40N,106W	40.5	16	1	2.5 (16)	2200	4.4°,4.8°	PAC	DB	60°(2,m)	op	(17)
United Kingdom	MST	—	~50	12	1	5	5200	3.6°	PAY	DB	5°,10°(2)	pl	(18)
Urbana/USA	MST	40N,88W	40.9	6	10	1	2000	(<3°)	PAD	DB	1.5°(1),2.5°(2)	op	(19)

mode: IS = incoherent scatter (thermosphere, may include mesosphere)
MST = mesosphere,stratosphere,troposphere
ST = stratosphere,troposphere

antenna:
configuration: PA = phased array
PAC = phased array, coaxial-collinear dipoles
PAD = phased array, dipoles
PAY = phased array, Yagis

mode: DB = Doppler beam swinging
SA = spaced antenna (interferometer)

steerability: 15°(2) = zenith angle 15° in 2 orthogonal planes (and zenith)
15°(m) = multiple position out to 15° zenith angle (and zenith)

status: op = operational
op/rt = routine operation (continuous)
ce = under construction
pl = planned

ref.: (1) Woodman+); (2) Vincent et al., 1982; (3) Brosnahan et al.+); (4a) Röttger et al.+); (4b) Hagfors et al., 1982; (5) Balsley+); (6) Koshy+); (7) Woodman and Guillén, 1974, Woodman and Farley+); (8) Crochet+); (9) Rastogi+); (10) Kato+); (11) Peters+); (12) Strauch et al., 1983, Strauch+); (13) Balsley et al., 1980, Balsley et al.+); (14) Glass+); (15) Watkins+); (16a) Röttger et al., 1978; (16b) Czechowsky et al.+); (17) Green et al., 1975, Green+); (18) Hall+); (19) Røyrvik and Goss+)

+) = in: Bowhill (1984), Handbook for MAP 9.

Some typical characteristics of MST VHF radars used for vertical profiling

peak power: 50 – 500 kW
antenna aperture: 1000 – 10000 m^2

best resolution:
altitude: 100 m
time: 10 s
accuracy: U, V ≤ 1 ms^{-1}
W ≤ 0.1 ms^{-1}

measure vertical profiles of:

U; V; W
clear air turbulence and waves
stability, reflectivity
→ tropopause, frontal zones,
(potential temperature)

MST RADARS ARE CAPABLE TO OBSERVE:

(1) Reflectivity Structure:

(a) morphology of turbulence,
e.g., intensity, intermittency, thickness and anisotropy

(b) stability index (coherency $\propto \partial\theta/\partial z$),
e.g., air mass mixing zones, inversion layers and tropopause

(2) Velocity Field:

(a) mean horizontal and vertical velocities u,v,w,
e.g., winds and convective processes

(b) fluctuating (oscillating) velocities u',v',w',
e.g., gravity waves and turbulence

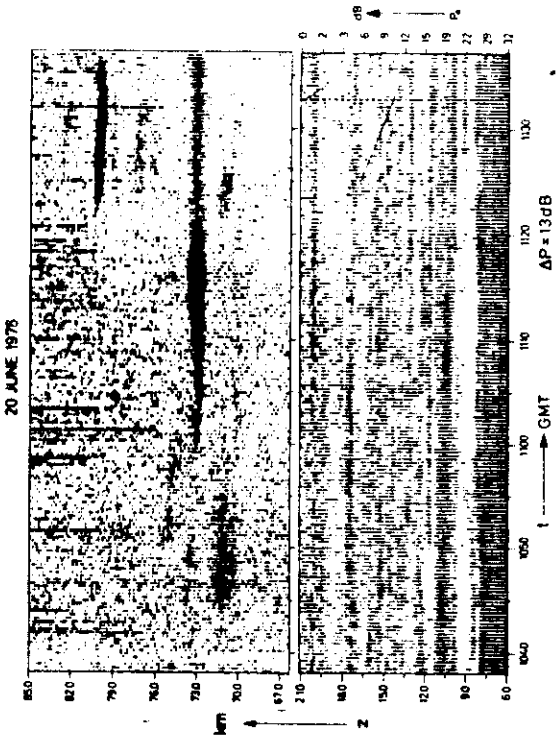

Example of a height time intensity plot of turbulence layers detected with a vertically beaming VHF radar in the upper troposphere (thin layers) and the mesosphere

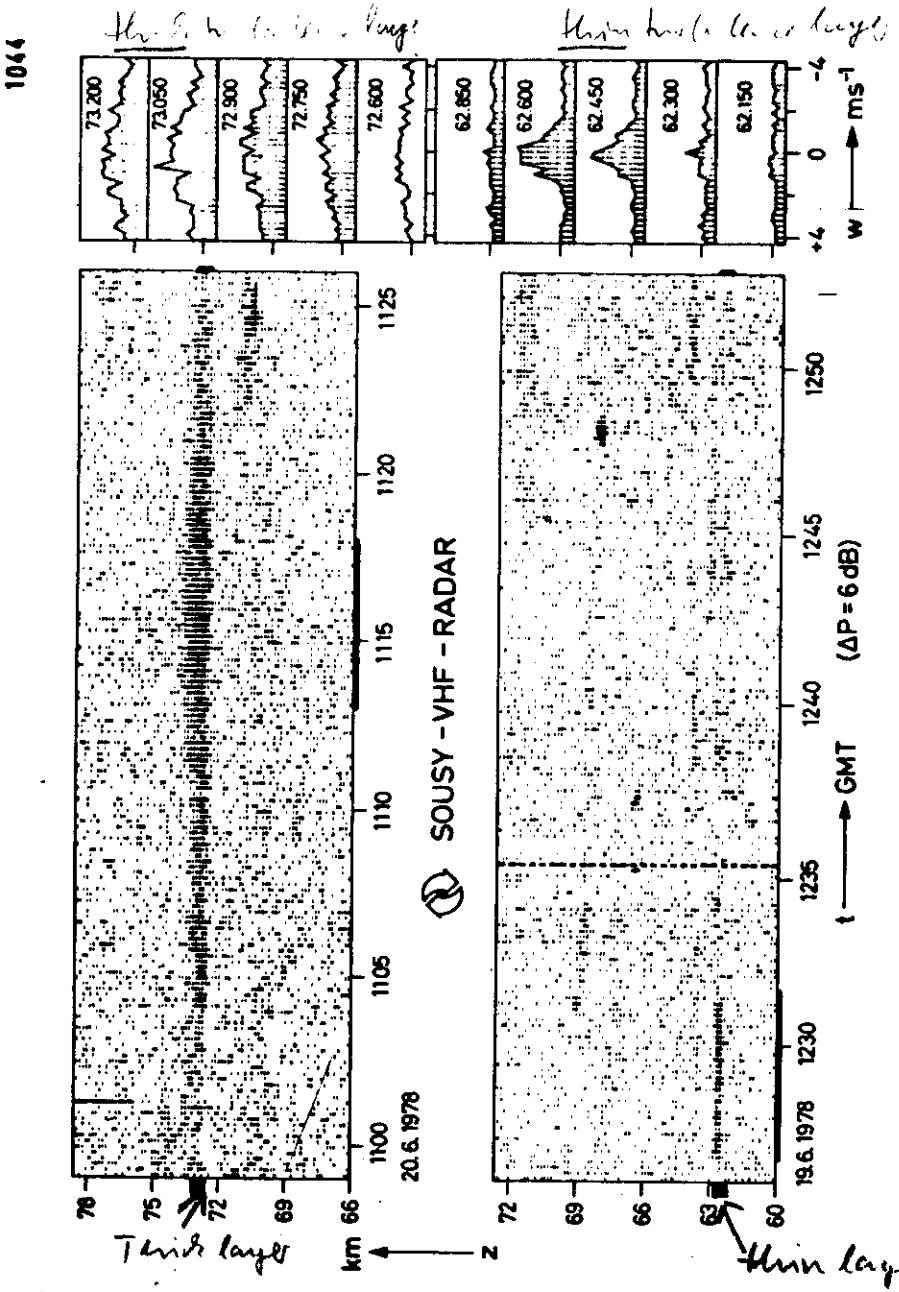

Thick turbulence layers have wide spectra and thin layers narrow spectra, according to turbulence theory.

5 JAN 1981

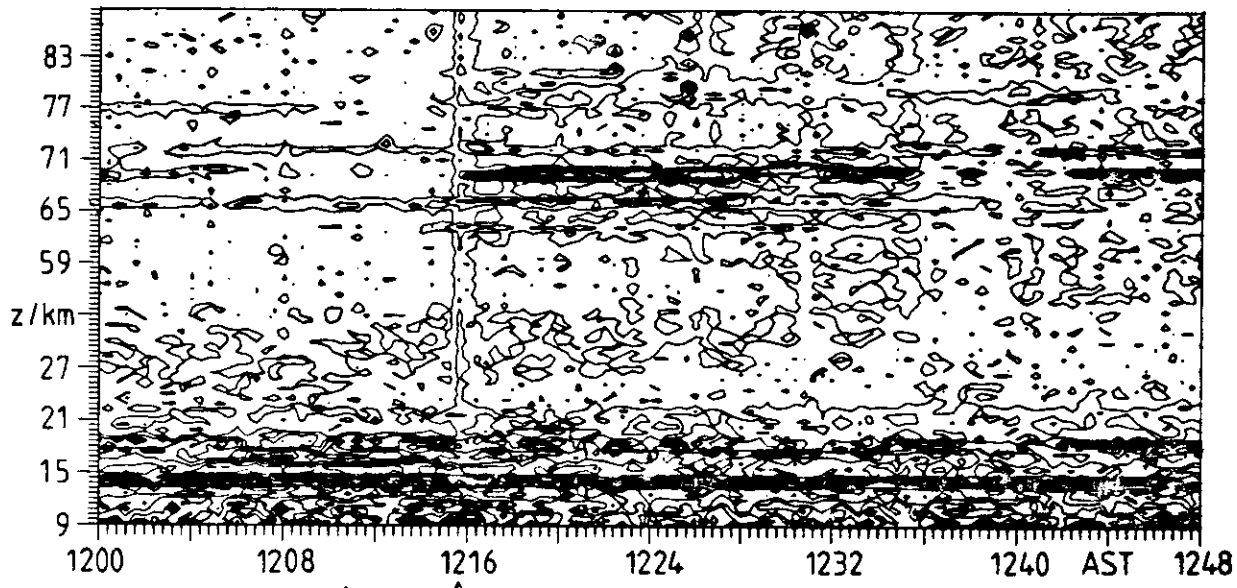

CONVECTIVE (IN)STABILITY

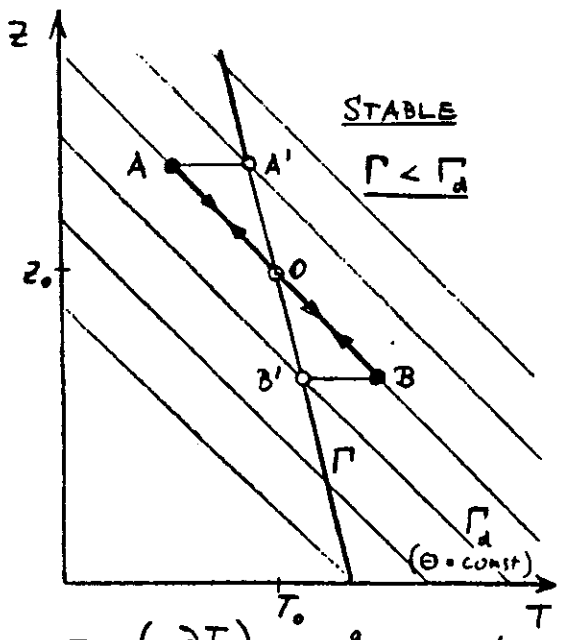

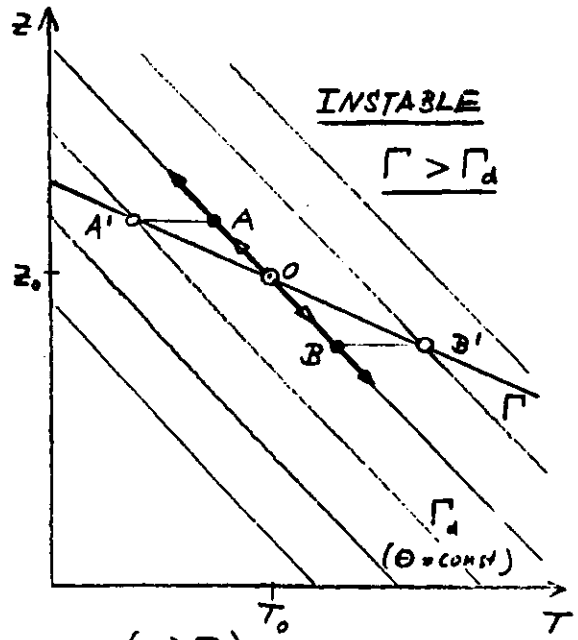

$$\Gamma_d = \left(-\frac{\partial T}{\partial z}\right)_{dry} = \frac{g}{c_p} = 9{,}8\ \frac{deg}{km}$$

↳ dry adiabatic lapse rate

$$\Gamma = \left(-\frac{\partial T_m}{\partial z}\right)_{measured}$$

↳ actual lapse rate

$$\Theta = T\left(\frac{p_0}{p}\right)^{0.286}$$

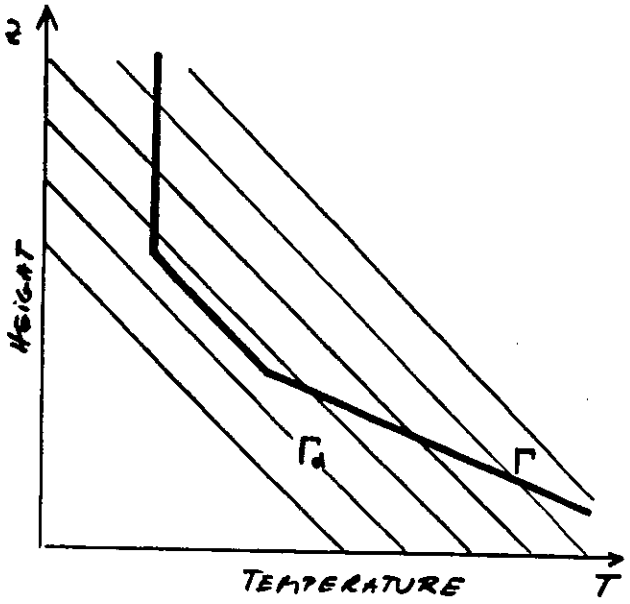

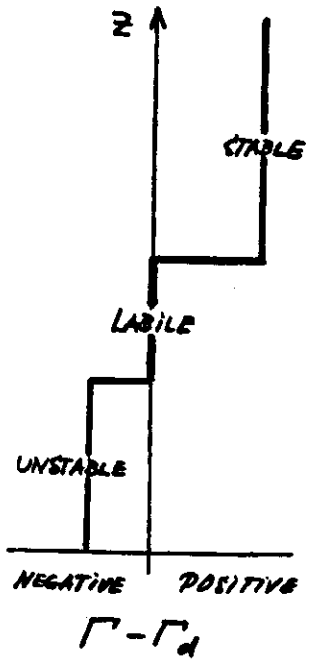

Shear Instability

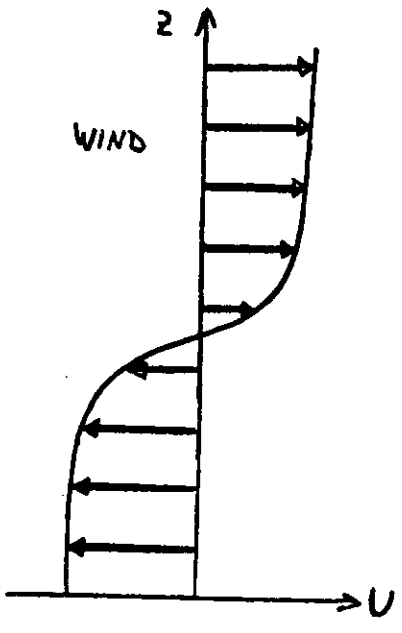

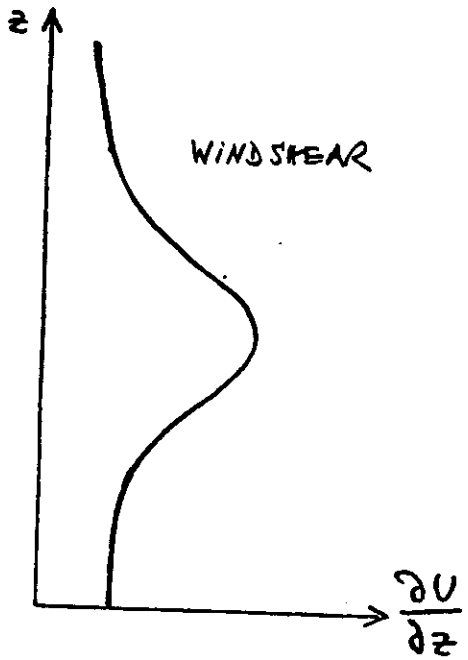

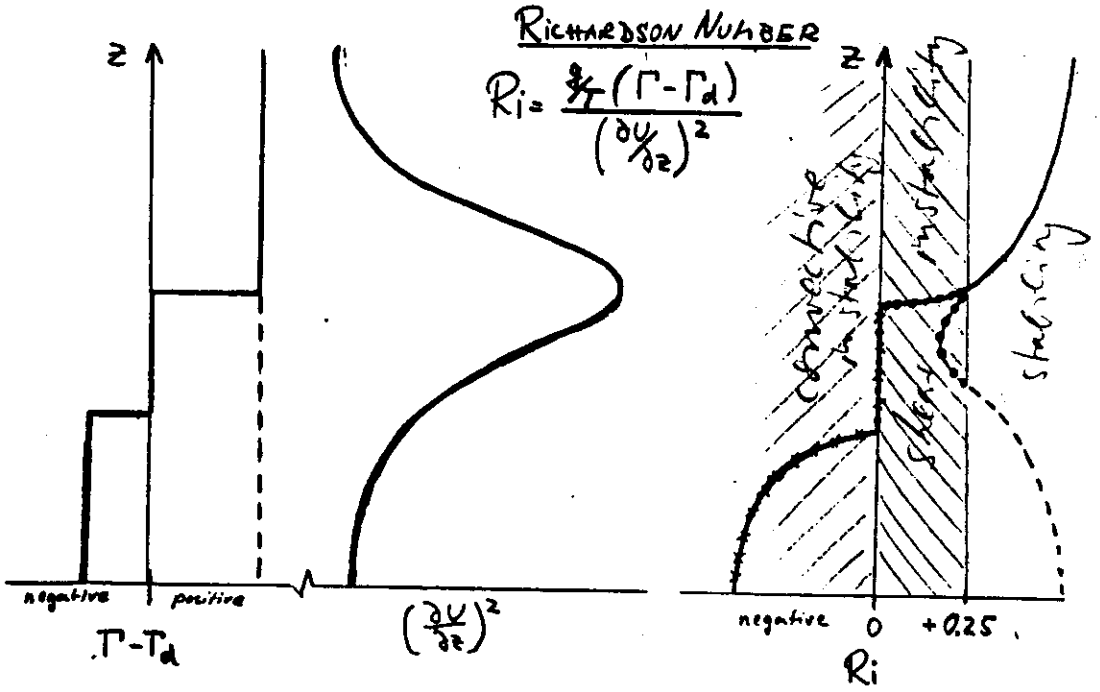

SHEAR INSTABILITY
(KELVIN-HELMHOLTZ-INSTABILITY)

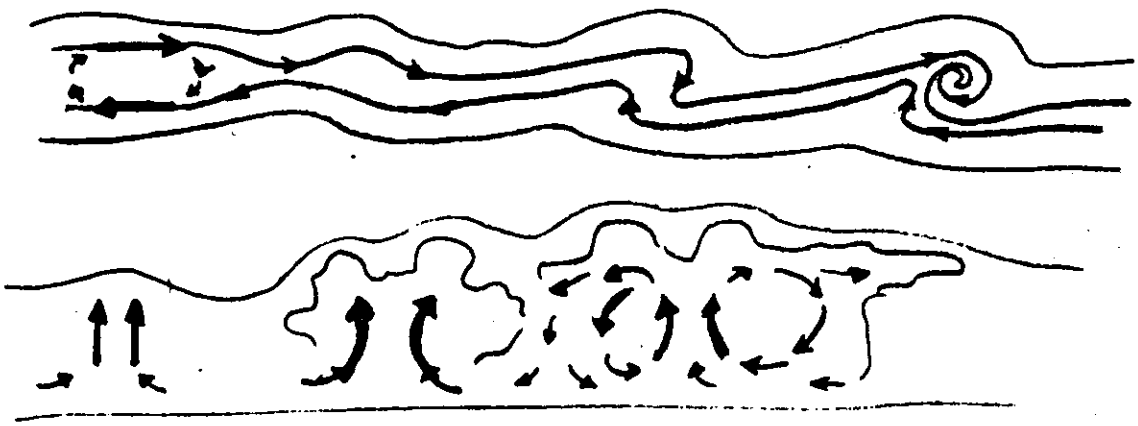

CONVECTIVE INSTABILITY

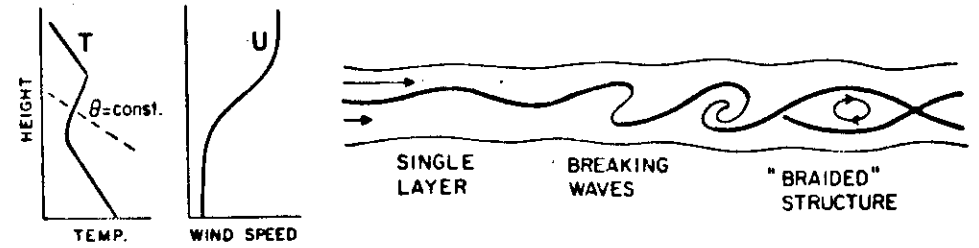

$$Ri = \frac{N^2}{\left(\frac{\partial u}{\partial z}\right)^2}$$

Breaking of gravity wave, causing CAT's ages turbulence shutdowns and double and multiple sheets (vertical temperature gradients) which persist after the decay of the originating turbulence layer. The persistence is a measure of atmospheric stability.

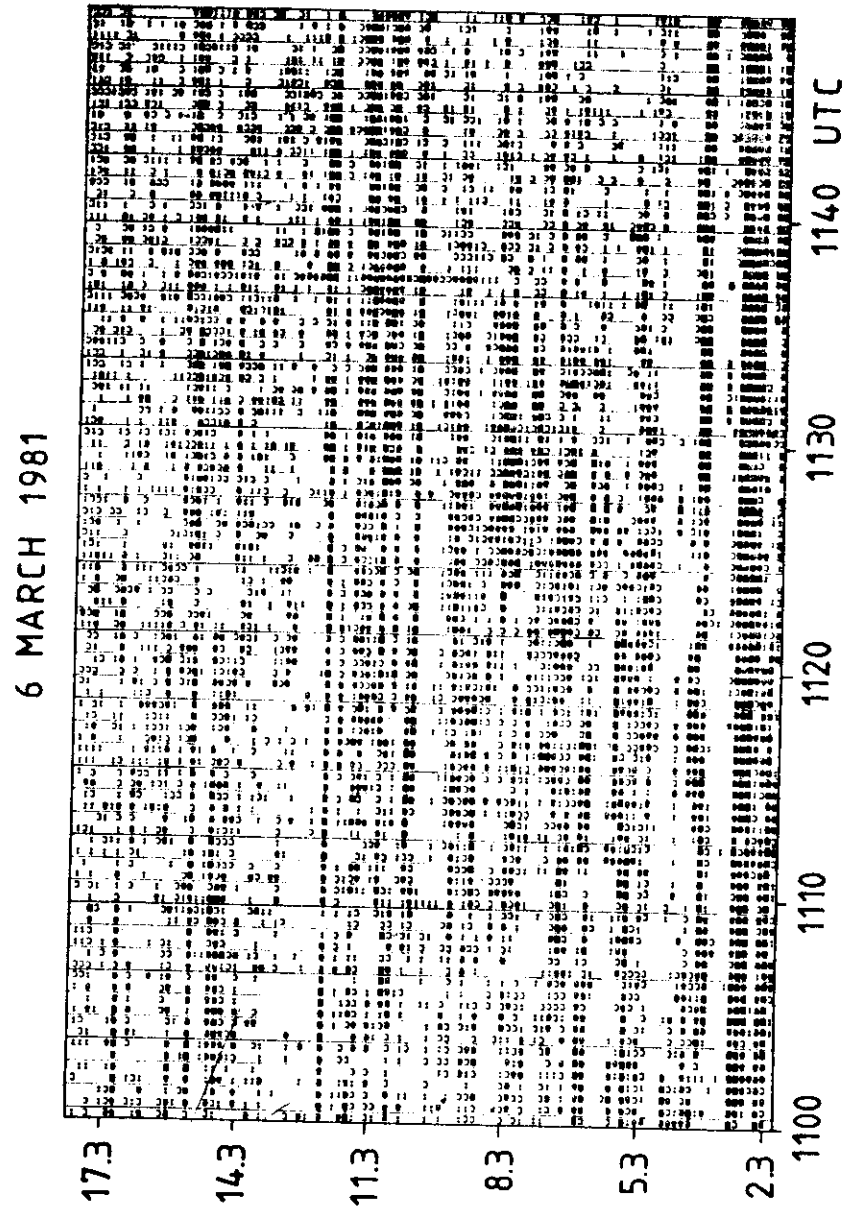

Sheets (temperature steps) observed with a vertically beaming VHF radar.

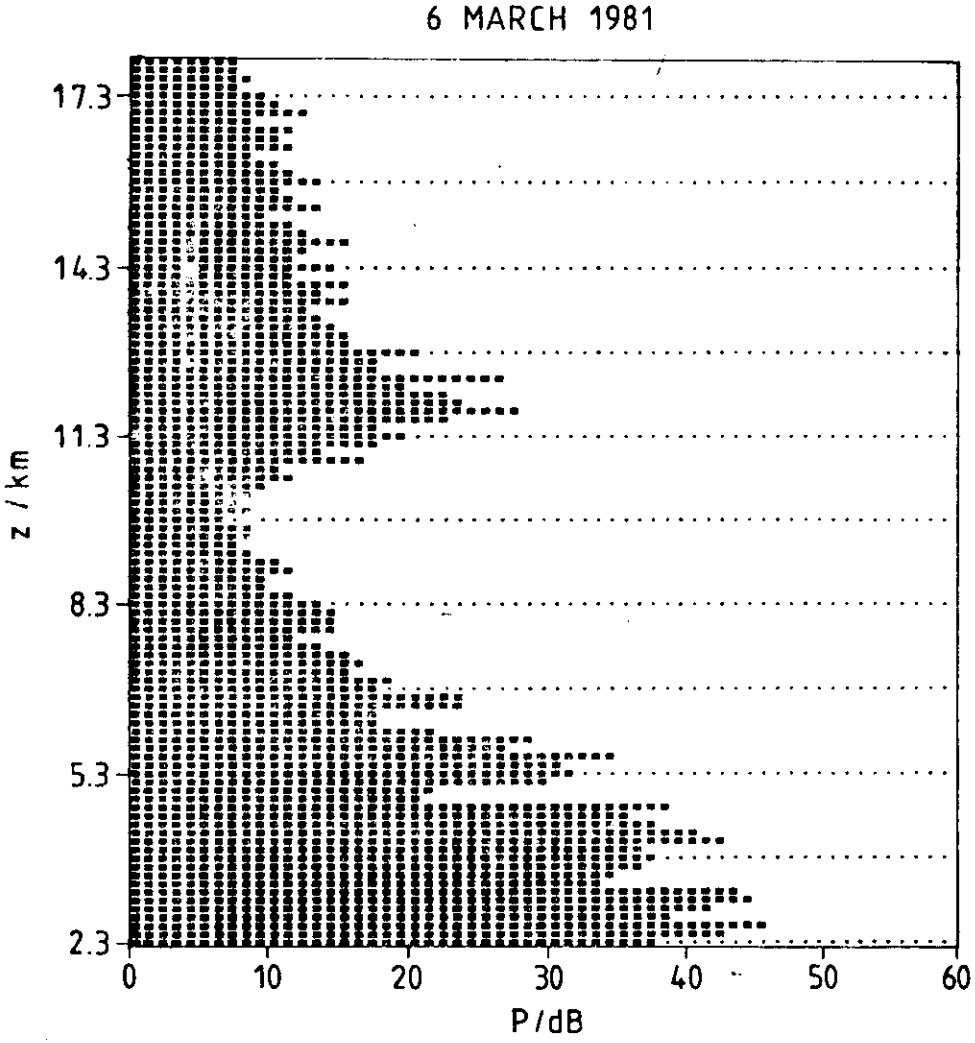

Typical high-resolution power profile measured (1 h average) with a vertical beaming VHF radar

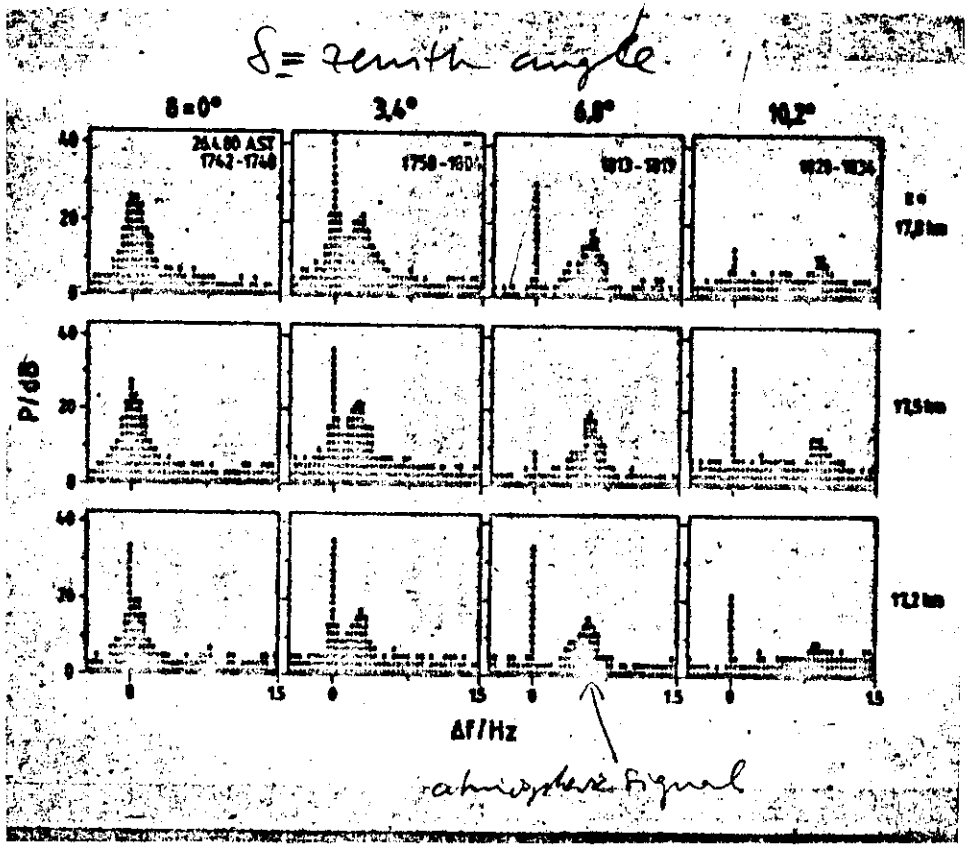

Decrease of signal power with increasing zenith angle, caused by the aspect sensitivity of the scattering/reflecting sheets and layers of turbulence

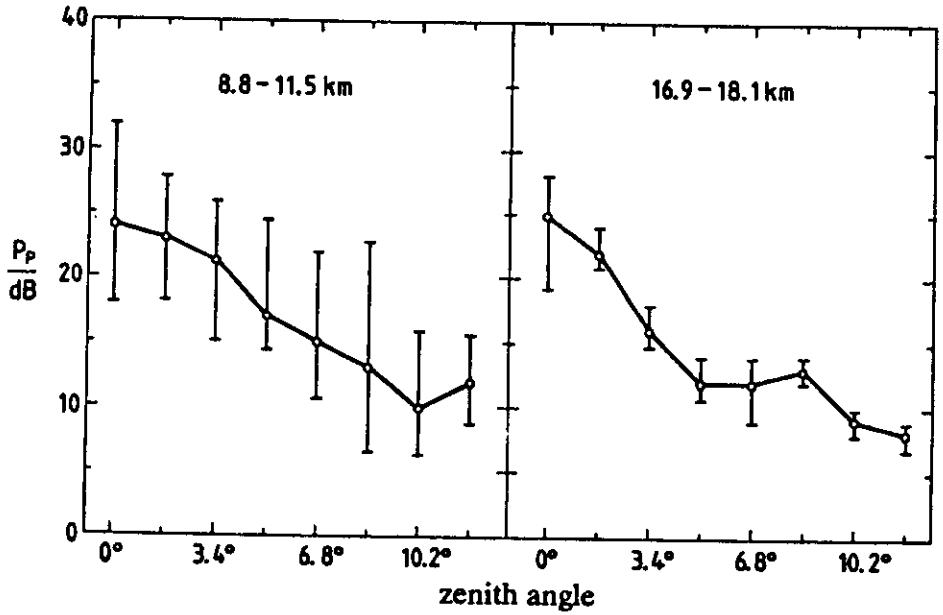

Signal power as function of zenith angle; the decrease with zenith angle is due to the aspect sensitivity

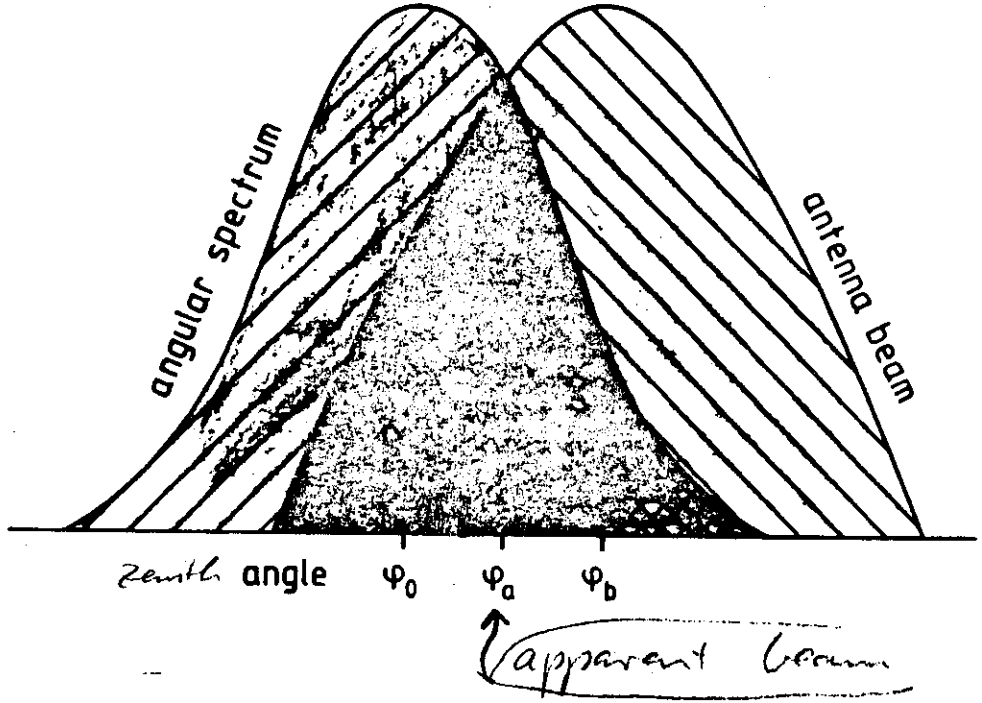

Because of the aspect sensitivity (given by the angular spectrum centered around the zenith angle φ_0) the antenna beam (direction φ_b) does apparently point to the direction φ_a.

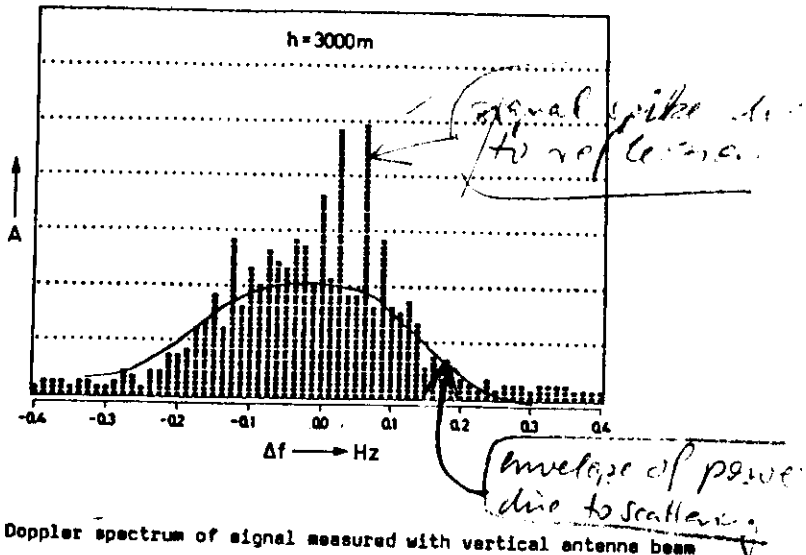

Doppler spectrum of signal measured with vertical antenna beam and 150 m height resolution, averaged over 8 min (from Röttger, 1980).

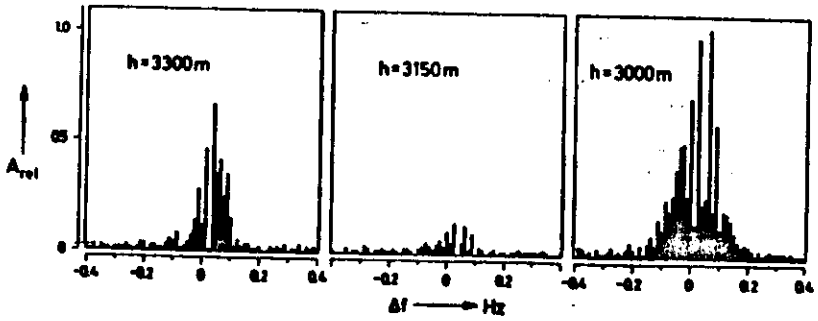

Doppler spectra computed from an 80 s time series.

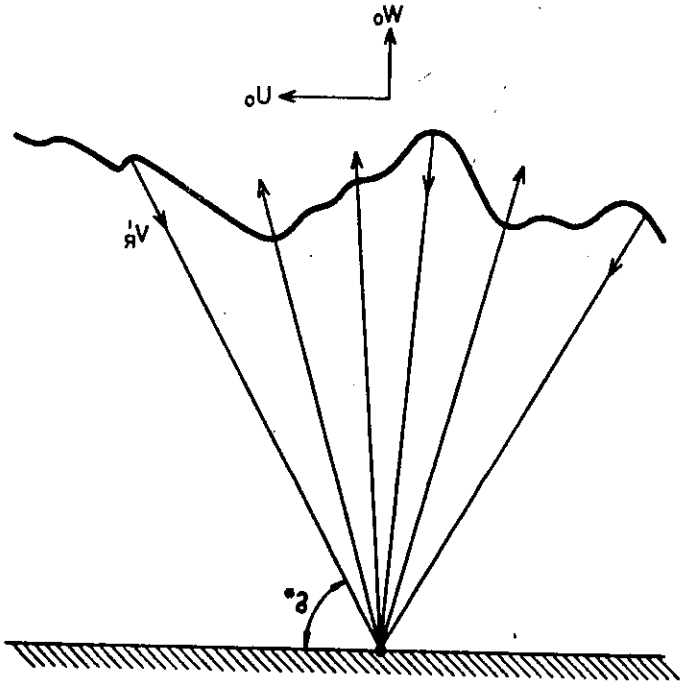

Reflection from different parts of a rough surface, moving with slightly different radial velocity. This causes the spikes on the power spectrum.

Evidence for Partial Reflection of VHF Radar Signals

1. Assuming pure volume scattering, it is deduced from the observed high radar echo power that the mean refractive index structure constant C_n^2 in several cases must be 1–2 orders of magnitude larger than currently accepted values or another mechanism than scattering has to be considered.

2. The correlation times of radar signals often are up to minutes in contrary to expected correlation times of a few seconds when assuming turbulence scattering.

3. The radar echo power is proportional to the correlation time which is just opposite to turbulence theory.

4. The intensity variations of radar echoes often are quasi-periodic (periods of some ten seconds). This can be explained by interference or focussing due to reflection at thin layers or patches of enhanced humidity or temperature variations which are influenced by atmospheric waves.

5. Peak radar echoes are much weaker (up to 20 dB) and not as structured when swinging the radar beam from the vertical to off-vertical (12.5° zenith angle). This points to reflection at vertical incidence into rough, horizontally stratified layers.

The layers are estimated not to exceed a few ten meters in vertical extent. The vertical gradient of refractive index has to be about $10^{-7}m^{-1}$. The horizontal dimension of the stratified layers must be at least several 100 m.

Evidence for Partial Reflection of VHF Radar Signals

6. The amplitude distributions of strong tropospheric radar echoes cannot be fitted to a Rayleigh distribution which would be expected for turbulence scattering. A better fit is possible when assuming that the signals contain a constant, partially reflected part. Phase distributions are not random (i.e. phases equally distributed between 0 and 2 π), but also indicate consistent contributions from partial reflection.

7. Doppler spectra of strong radar echoes do not fit to a Gaussian shape which is anticipated if one assumes turbulence velocities to be normally distributed. High resolution spectra indicate strong spikes superimposed on Gaussian shaped spectra which must be caused by partial reflection.

8. The radar echo power P often is found not to be proportional to the antenna area A which is expected for turbulence scattering. A better fit is obtained if $P \propto A^k$ with $1 < k \leq 2$, which is expected if the signal contains contributions from partial reflections.

9. The spatial coherence of the echo pattern on the ground often is much greater than expected for turbulence scattering.

Conclusion

It appears reasonable that partial reflection also should be considered to explain VHF radar signals (at quasi-vertical beam pointing) from the stratosphere and mesosphere. According to considerations on transhorizon propagation (Beckman and Spizzichino, 1963), the most appropriate mechanism responsible for VHF radar echoes from the troposphere, stratosphere and mesosphere is proposed to be a composition of (1) specular (partial) reflection at rather stable stratified layers, (2) diffusive reflection at rough layers and (3) scattering from turbulence.

Since partial or diffusive reflection often appears to occur, VHF radar systems, due to the longer wavelengths; are more favorable than higher frequency radars to detect these layers in the atmosphere and to make use of the strong radar echoes to investigate the dynamics of the lower and middle atmosphere.

Interferometer applications of VHF radars

What can be gained as compared to the conventional application of Doppler and drift measurements ?

* measure incidence angle of echoes
* improve (correct) the vertical and horizontal velocity measurements
* measure parameters of atmospheric gravity waves
* track turbulence patches and deduce their vertical and horizontal velocities
* increase spatial extent (horiz.) of simultaneously sensed volume
* measure inhomogeneity and fine structure in the horizontal plane (angular spectrum)

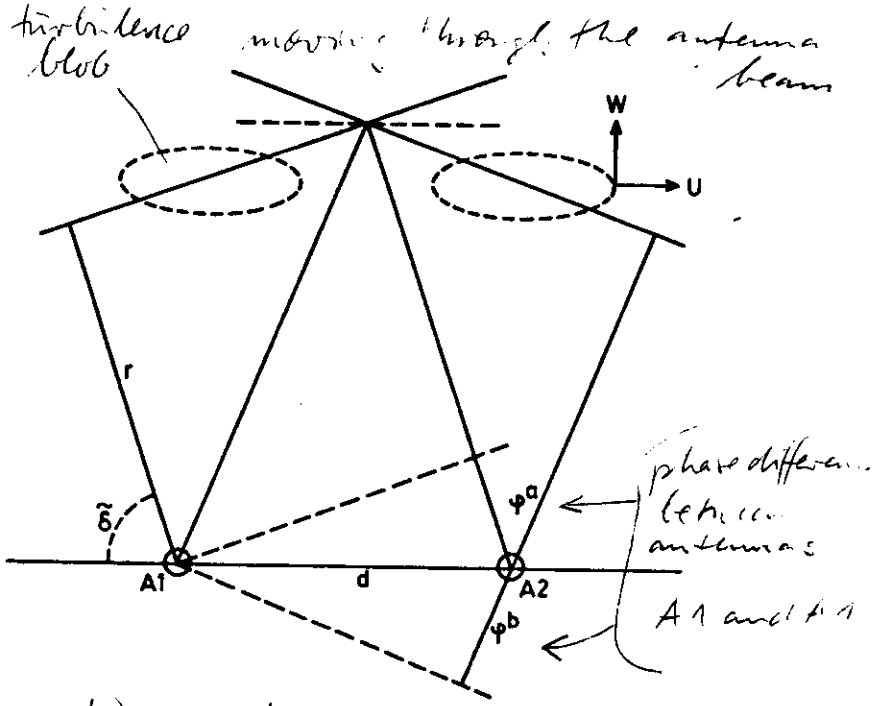

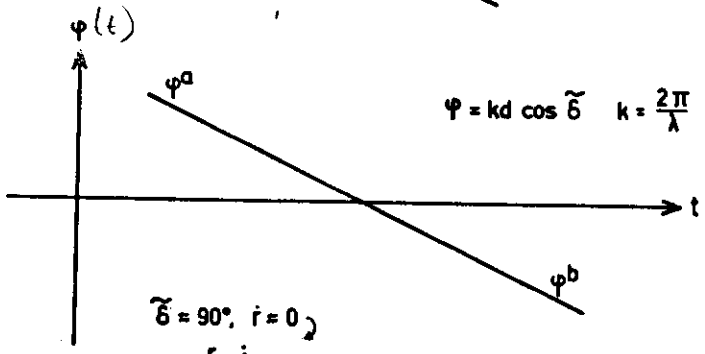

$\varphi = kd \cos\tilde{\delta} \quad k = \frac{2\pi}{\lambda}$

$\tilde{\delta} = 90°,\ \dot{r} = 0$

$U = \frac{r}{kd}\dot{\varphi}$

$\omega = 2k\,(U \cdot \cos\tilde{\delta} + W \cdot \sin\tilde{\delta})$

the phase difference φ varying as a function of time indicates that a scattering/reflecting turbulence blob moves through the antenna beam with the horizontal velocity U.

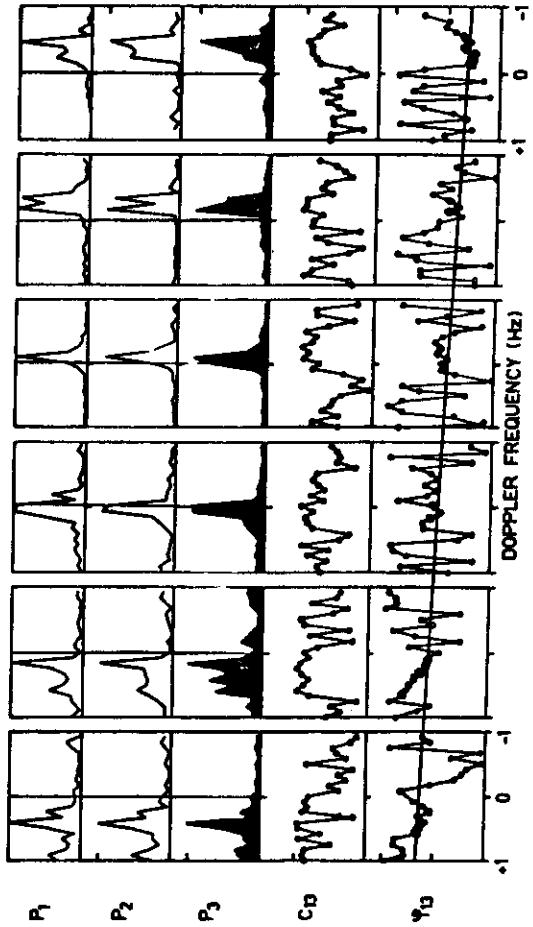

Power spectra P of signals received at 3 spaced antennas and the coherence C_{13} and the phase φ_{13} between antennas 1 and 3. The change from positive to negative Doppler shift and the phase variance indicate a turbulence blob moving horizontal and vertical with respect to the

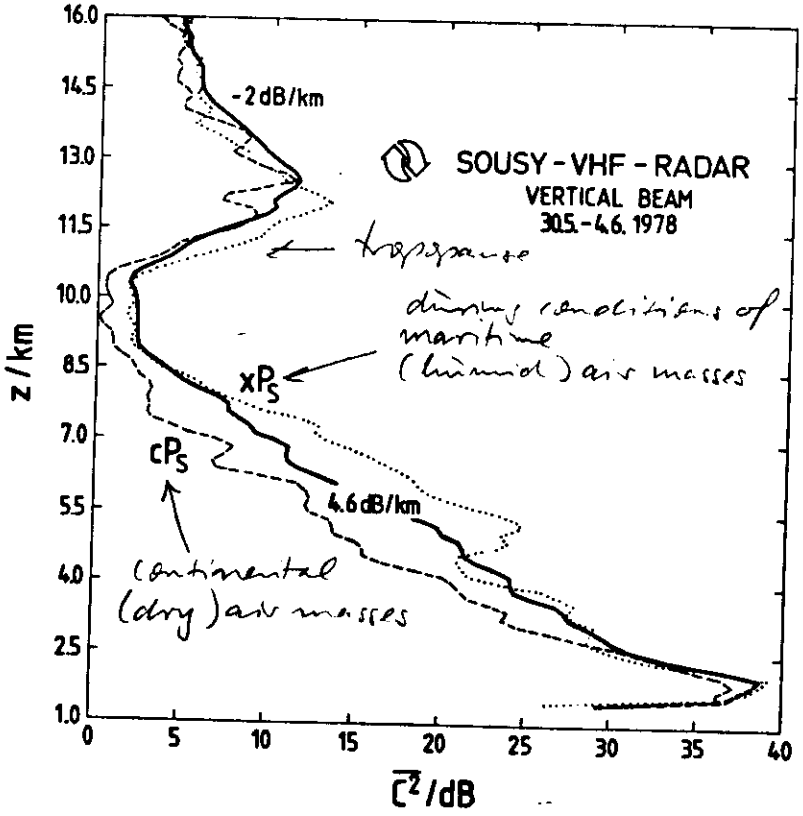

Effective reflectivity $\bar{C}^2$ ($\sim P \cdot z^2$)

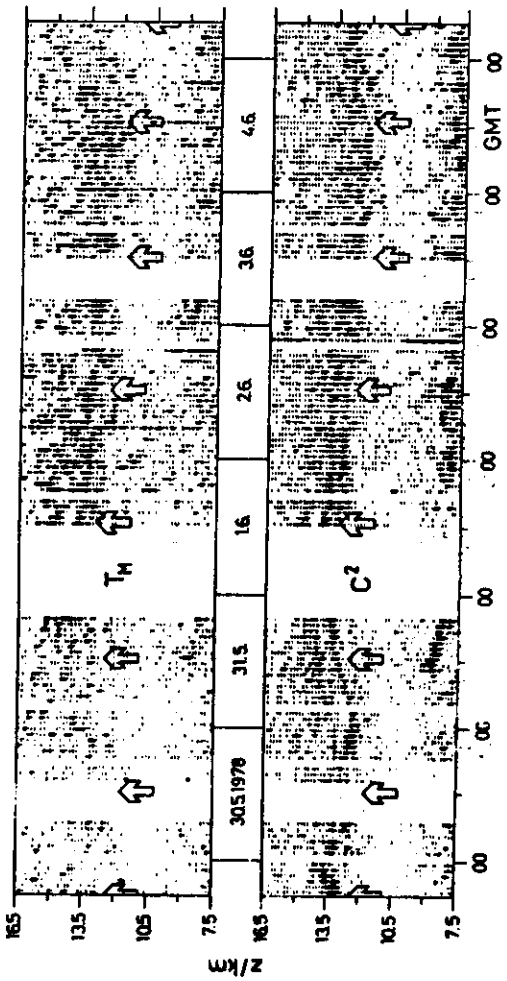

Tropopause height detected with radar Height - time - intensity plots of effective reflectivity C^2 and radiosonde data (arrows).

13429

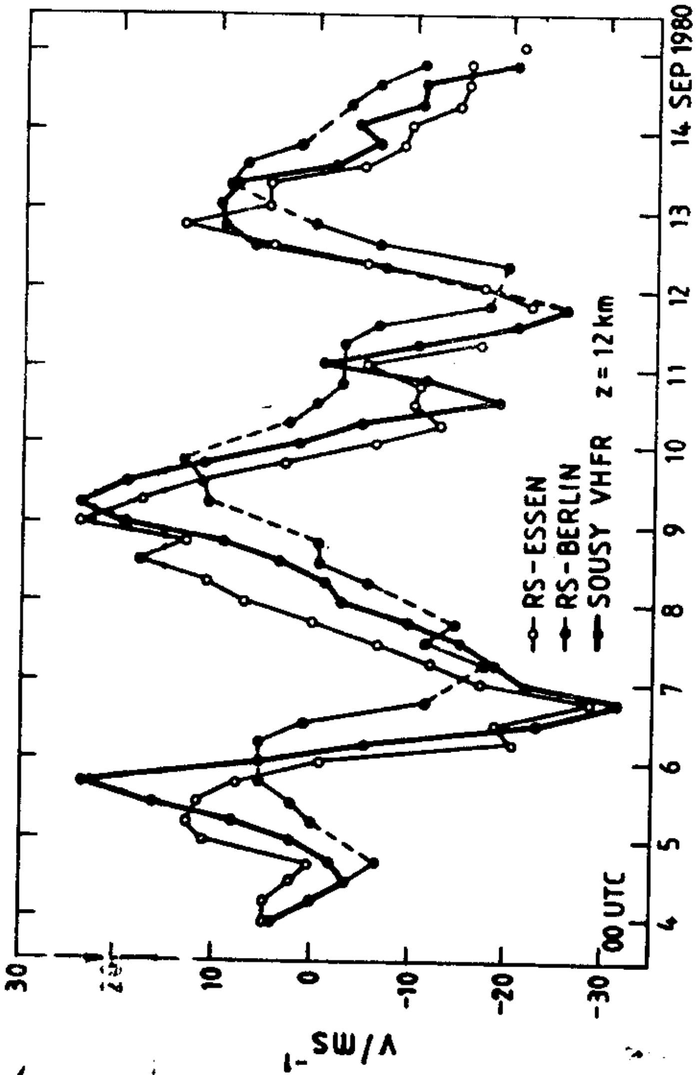

Meridional velocity, oscillating due to the passage of tropospheric extratropical cyclones.

28

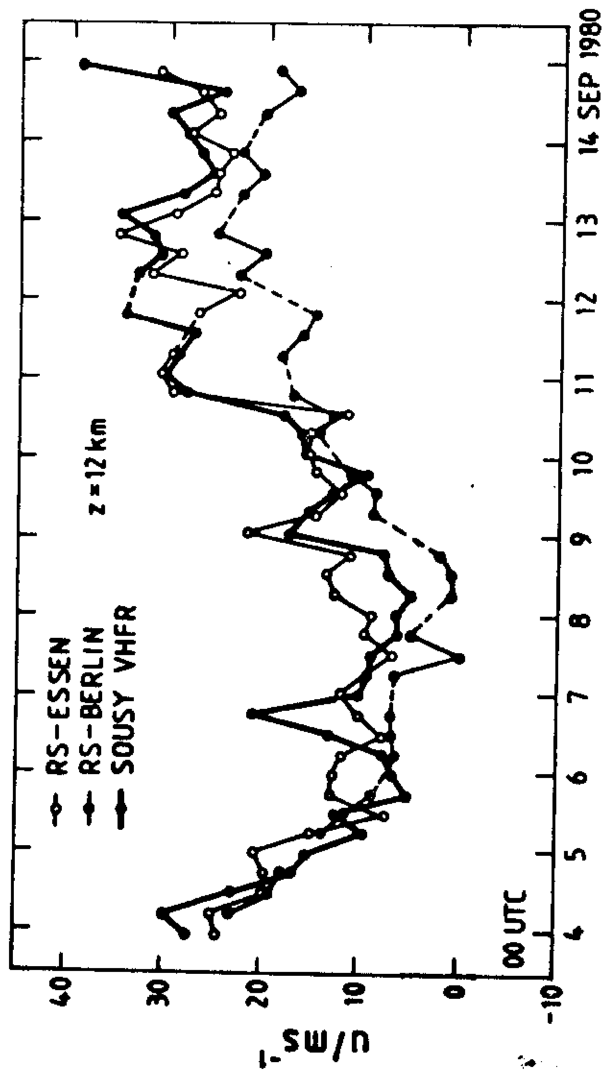

Zonal velocity in eastward direction (westerly winds) indicating that tropo= spheric Rossby waves could propagate into the Stratosphere.

29

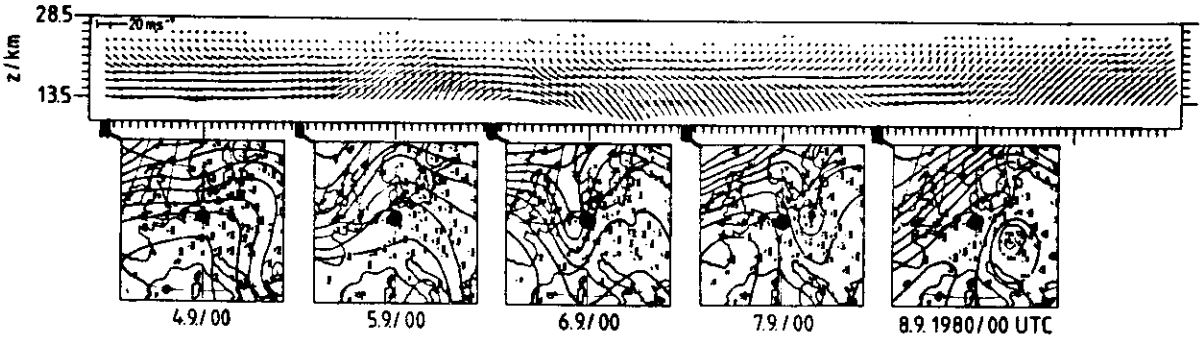

30

· Weather charts of 300 mb level and vector plot of stratospheric winds measured with radar. The stratospheric winds reflect the winds in the upper troposphere, but decrease in amplitude with height, because their zonal wavenumber ($k \approx 8$) is too large to allow propagation into stratosphere.

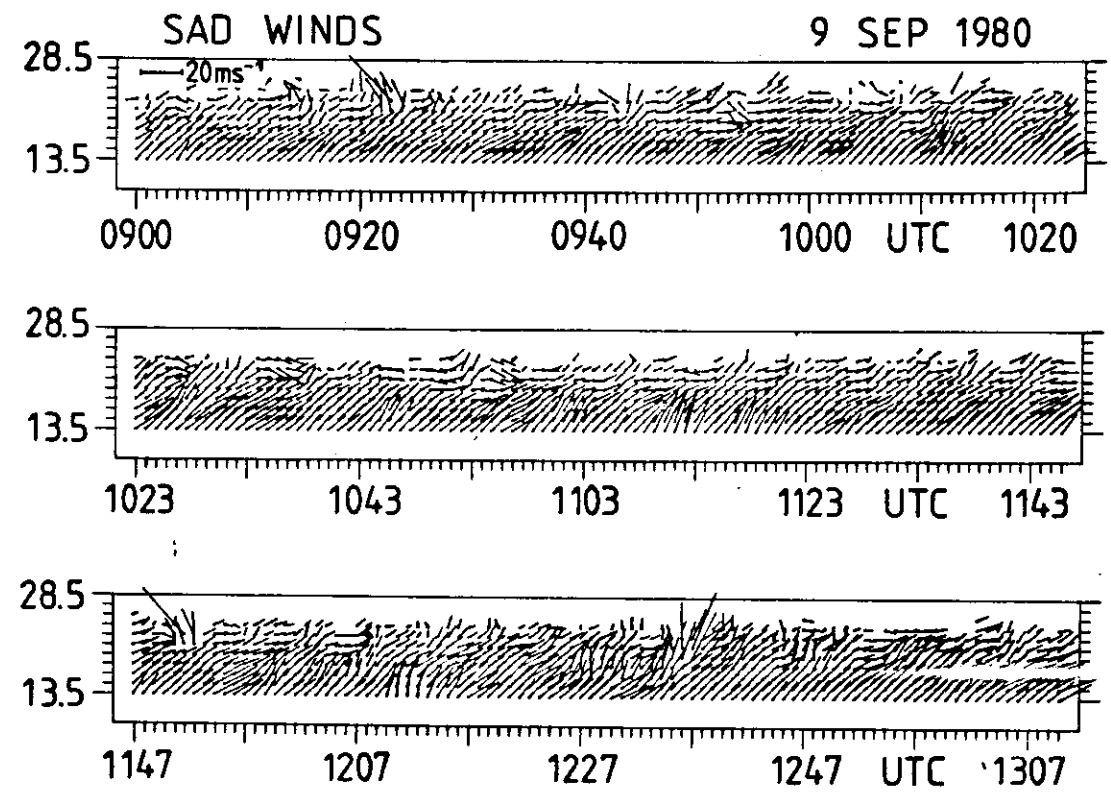

Fluctuations of meridional wind in the lower stratosphere

31

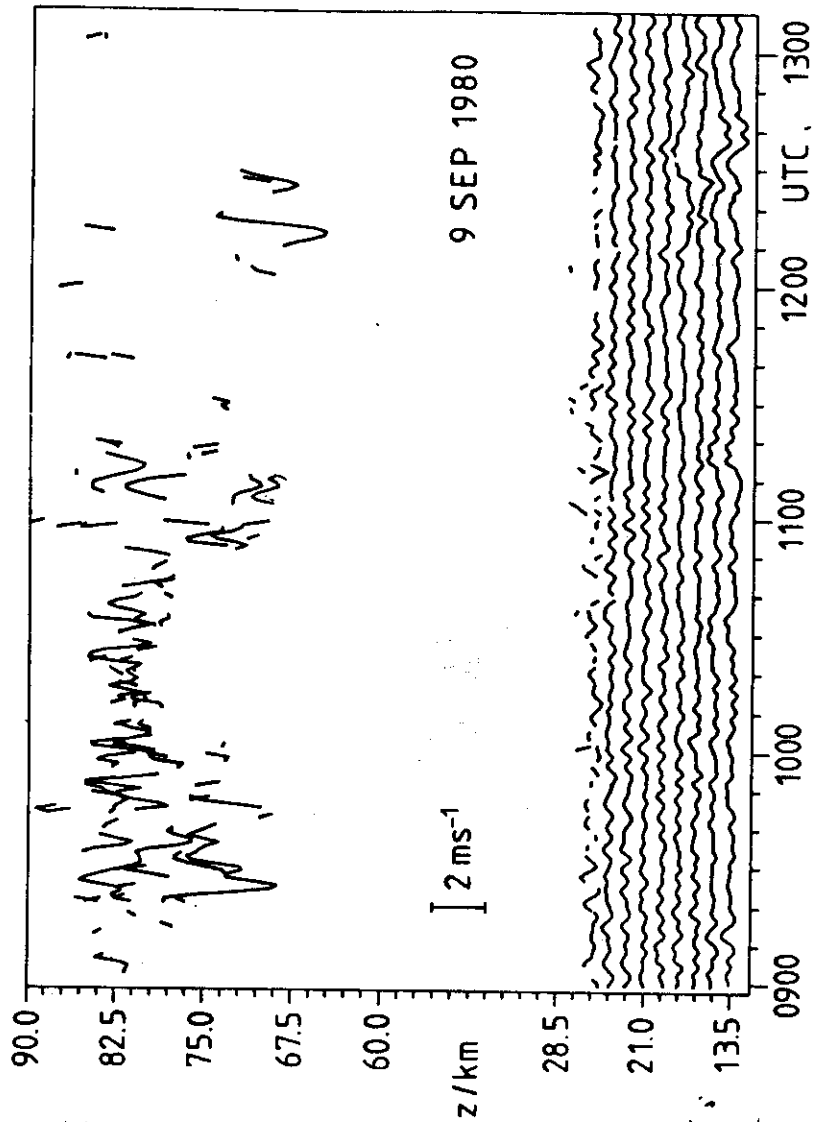

Vertical velocity variations in the mesosphere and lower thermosphere indicating internal gravity waves

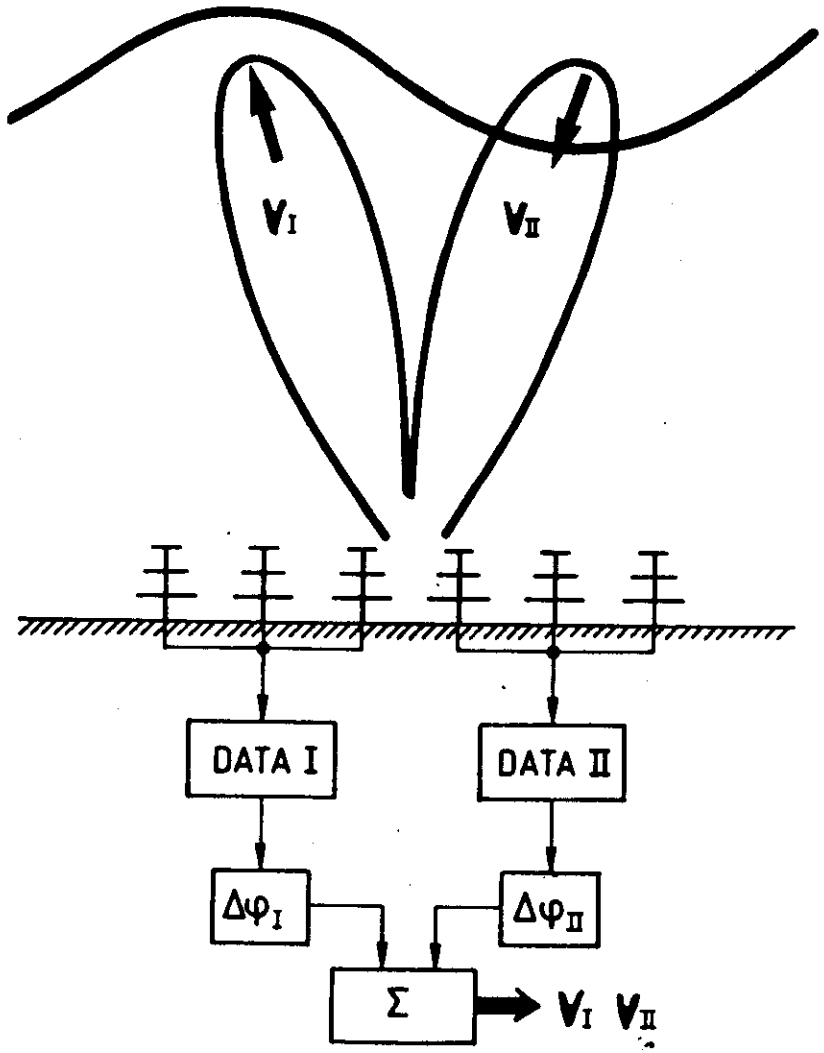

Two-beam interferometer technique to measure parameters (horizontal phase velocity, ...) of gravity waves

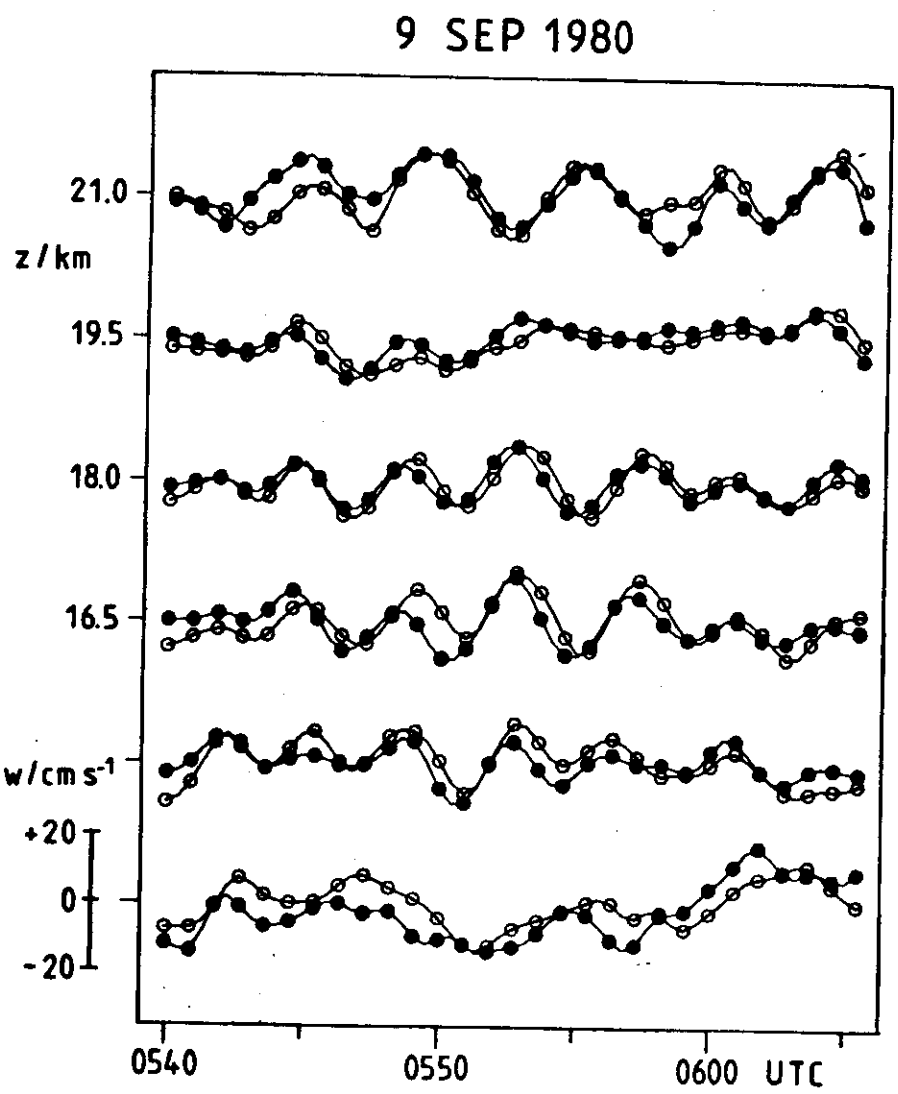

Vertical velocity oscillations due to atmospheric gravity wave, measured at two beam directions. The phase shift between the oscillations indicates a horizontally propagating wave

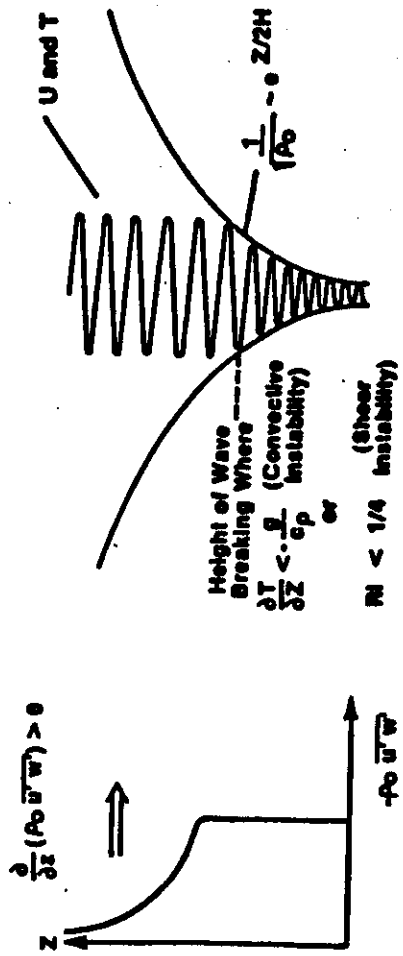

The momentum flux $\rho \overline{w'v'}$ due to gravity waves is constant with height, if the waves are not breaking (attenuation not included).

$\overline{w'u'}$ should follow $\exp(z/4)$ if no wave reflection, attenuation or breaking takes place. At periods 4–6 min, obviously $\overline{w'u'}$ decreases above 20 km, being indication of breaking (?)

Spectra of vertical velocity $\overline{w'}$, horizontal velocity $\overline{u'}$ and cross product $\overline{w'u'}$, being a measure for momentum flux. Spectral peaks at 4–6 min are due to gravity waves.